

Synthesis, characterization and catalytic properties of SAPO-34 synthesized using diethylamine as a template

Guangyu Liu^{a,b}, Peng Tian^a, Jinzhe Li^{a,b}, Dazhi Zhang^{a,b}, Fan Zhou^{a,b}, Zhongmin Liu^{a,*}

^a Laboratory of Applied Catalysis, Dalian Institute of Chemical Physics, Chinese Academy of Sciences, 457 Zhongshan Road, Dalian 116023, PR China

^b Graduate University of the Chinese Academy of Sciences, Beijing 100049, PR China

Received 26 April 2007; received in revised form 9 July 2007; accepted 9 July 2007

Available online 19 July 2007

Abstract

SAPO-34 molecular sieve was successfully synthesized using diethylamine (DEA) as a template. The influence of template concentration and silica concentration on the synthesis were investigated. Pure SAPO-34 could be obtained when $n(\text{DEA})/n(\text{Al}_2\text{O}_3) \geq 1.5$ and $n(\text{SiO}_2)/n(\text{Al}_2\text{O}_3) > 0.1$ in the synthesis gel. Further increase of DEA concentration in the starting gel [$n(\text{DEA})/n(\text{Al}_2\text{O}_3) > 3$] has a negative effect on both crystallinity and crystal yield. The products were characterized by XRD, XRF, SEM, NMR, FT-IR, TG-DTA and nitrogen adsorption techniques. It was found that SAPO-34 synthesized with DEA as a template has the characteristic of high silicon incorporation and exhibits good thermal and hydrothermal stability. The catalytic performance of SAPO-34 was tested by methanol-to-olefin (MTO) reaction and high olefins ($\text{C}_2\text{H}_4 + \text{C}_3\text{H}_6$) selectivity was obtained.

© 2007 Elsevier Inc. All rights reserved.

Keywords: Synthesis; SAPO-34; Diethylamine; Hydrothermal stability; Methanol-to-olefin (MTO)

1. Introduction

Aluminophosphate (AlPO) and silicoaluminophosphate (SAPO) molecular sieves were firstly reported by Union Carbide in 1980s [1,2]. The structures of AlPOs and SAPOs cover a range of different structure types; some are analogous to certain zeolites such as SAPO-34 (CHA structure), but a large number have unique structures without analogous zeolite. Since the frameworks of AlPO molecular sieves are neutral, they usually have no actual catalytic capabilities. The substitution of silicon into the framework of AlPOs, i.e. SAPOs, result in the appearance of acidity and leads to their catalytic application [2]. Among SAPOs, small-pore SAPO-34 has received great attention in recent years due to its high selectivity to olefins in methanol-to-olefin (MTO) reaction [3–5], and many research works have been reported relating to the synthesis and crystalliza-

tion mechanism [6–8], its catalytic properties in MTO reaction and reaction mechanisms [3,4,9–21].

It is well known that template plays important roles in the synthesis of molecular sieves, such as structure-directing, space-filling and charge-compensating roles [5,22,23]. One template may produce molecular sieves with different structures by varying the synthetic conditions; and one type of molecular sieve could also be synthesized in the presence of different organic templates [22]. The elemental composition, local microscopic structure and morphology of one specific molecular sieve may change with the use of different templates. Therefore, the catalytic performance and adsorption properties of the obtained materials may be different.

Many organic amines can be used as templates for the synthesis of SAPO-34, including tetraethylammonium hydroxide (TEAOH) [15,23,24], dipropylamine [24], isopropylamine [24], piperidine [25], morpholine [6,8,23,26], triethylamine (TEA) [7,27], and diethylamine (DEA) [28,29], etc. Up to now, research on the synthesis of SAPO-34 using DEA as a template is relatively scarce.

* Corresponding author. Tel.: +86 411 84685510; fax: +86 411 84691570.

E-mail address: liuzm@dicp.ac.cn (Z. Liu).

The present paper reports the synthesis of SAPO-34 synthesized with DEA as a template in detail. Many techniques such as XRD, XRF, SEM, NMR, FT-IR, TG-DTA and nitrogen physisorption were employed to characterize the obtained SAPO-34. The catalytic performance of samples in MTO reaction was also tested.

2. Experimental

2.1. Synthesis

SAPO-34 was synthesized by a hydrothermal method from a gel with molar composition of (0–4.0)DEA: (0–0.8)SiO₂:1.0Al₂O₃:0.8P₂O₅:50H₂O. The sources for Al, P and Si were pseudoboehmite, 85% phosphoric acid and silica sol (25%), respectively. The gel was sealed in the autoclave and then heated at 200 °C for 48 h. After crystallization, as-synthesized sample was obtained after filtration, washing, and drying at 120 °C for 4 h. Calcination was carried out at 550 °C for 5 h to remove organic template.

SAPO-34 was also synthesized with TEA as a template for comparison. The gel molar composition is 3.0TEA: (0.1–0.8)SiO₂:1.0Al₂O₃:0.8P₂O₅:50H₂O. All the sources and synthesis process are the same as above. The crystallization conditions were 200 °C and 24 h.

2.2. Characterization

The powder XRD pattern was recorded on a Rigaku D/MAX-γB X-ray diffractometer with Cu Kα radiation ($\lambda = 0.15418$ nm). The chemical composition of the sample was determined with a Philips Magix-601 X-ray fluorescence (XRF) spectrometer. The crystal morphology was analyzed by scanning electron microscopy (SEM, KYKY-AMRAY-1000B). ²⁹Si MAS NMR spectroscopy measurement was conducted at resonance frequencies of 79.41 MHz, using a Varian Infinity plus 400 WB spectrometer. The spinning rates of the samples at the magic angle were 4 kHz. The reference material for the chemical shift (in ppm) was 2, 2-dimethyl-2-silapentane-5-sulfonate sodium salt (DSS). FT-IR spectrum (resolution of 4 cm⁻¹) was measured using KBr containing pellet on a Bruker Tensor-27 IR spectrophotometer. The thermal analysis was performed on a Perkin–Elmer Pyris-1 TGA and DTA-7 analyzer with the temperature-programmed rate of 10 °C/min under air flow. The textural data were obtained by nitrogen adsorption measurement using a Micromeritics 2010 analyzer. Before analysis all samples were degassed at 350 °C under vacuum.

2.3. Catalyst testing

MTO reaction was carried out with a fixed-bed reactor at atmospheric pressure. 2.5 g of catalyst (20–40 mesh) was loaded into the reactor. The sample was pretreated in a flow of nitrogen at 550 °C for 1 h and then the temperature of reactor was reduced to 450 °C. The mixture (the

weight ratio of CH₃OH/H₂O was 40/60) was pumped into the reactor after nitrogen was turned off. The weight hourly space velocity (WHSV) was 4 h⁻¹. The products were analyzed on-line by a Varian GC3800 gas chromatograph equipped with a FID detector and a PoraplotQ-HT capillary column.

3. Results and discussion

3.1. Effect of synthesis conditions

3.1.1. Effect of template concentration

The effect of template concentration on the synthesis was investigated with the gel molar composition of *x*DEA:0.6SiO₂:1.0Al₂O₃:0.8P₂O₅:50H₂O. The XRD patterns of obtained samples are shown in Fig. 1. Without the template DEA, dense phase was formed. As *x*(DEA) increased to 0.5, the characteristic peaks of SAPO-34 appeared, but it co-crystallized with SAPO-11 [30]. Pure SAPO-34 crystal could be observed when *x*(DEA) ≥ 1.5. If the crystallization temperature was decreased to 180 °C, pure SAPO-11 can be synthesized in the range of 0.4 ≤ *x*(DEA) ≤ 0.8.

The chemical analysis given in Table 1 indicates that the silicon content in SAPO-34 rises with the increase of DEA

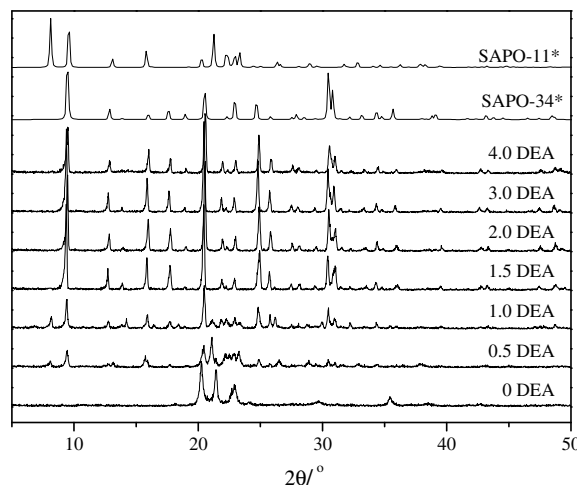


Fig. 1. XRD patterns of samples synthesized with different DEA concentration in the initial gel (*x*DEA:0.6SiO₂:1.0Al₂O₃:0.8P₂O₅:50H₂O).

Table 1
Effect of DEA concentration in the initial gel on synthesis

Sample	<i>x</i> (DEA)	Molar composition	Relative crystallinity (%)	Relative yield (%)
1	1.5	Si _{0.12} Al _{0.49} P _{0.40} O ₂	94	100
2	2.0	Si _{0.15} Al _{0.49} P _{0.36} O ₂	94	94
3	3.0	Si _{0.16} Al _{0.49} P _{0.35} O ₂	100	68
4	4.0	Si _{0.17} Al _{0.53} P _{0.30} O ₂	65	36

x(DEA):0.6SiO₂:1.0Al₂O₃:0.8P₂O₅:50H₂O.

concentration. Almost 1.4 times increase of $n(\text{Si})/n(\text{Si} + \text{Al} + \text{P})$ in the product was obtained with $x(\text{DEA})$ increasing from 1.5 to 4.0, which suggests that high template concentration in the gel can promote the incorporation of silicon into the framework. However, too much DEA in the gel would cause the sharp decrease of crystal yield and crystallinity. When the ratio of $x(\text{DEA}) = 4.0$, the relative crystallinity decreased to 65% and the relative yield was only 36%.

3.1.2. Effect of silica concentration

The effect of SiO_2 concentration in the initial gel on synthesis (the gel molar composition is $2.0\text{DEA}:\gamma(\text{SiO}_2):1.0\text{Al}_2\text{O}_3:0.8\text{P}_2\text{O}_5:50\text{H}_2\text{O}$) is shown in Fig. 2. It is found that amorphous boehmite instead of $\text{AlPO}_4\text{-34}$ was formed in the silica-free gel, which corresponds with the result that $\text{AlPO}_4\text{-34}$ can be only prepared in the presence of fluoride as reported in the literature [26]. In the range of $0 < \gamma(\text{SiO}_2) \leq 0.1$, SAPO-34 appeared together with boehmite. Pure SAPO-34 crystal was only obtained when $\gamma(\text{SiO}_2) > 0.1$.

Table 2 presents the chemical composition of the products and the level of silicon incorporation (ratio of silicon content in the as-synthesized sample to that in the reactant gel). When $\gamma(\text{SiO}_2)$ was equal to 0.05, the silicon incorporation level was 2.93. When $\gamma(\text{SiO}_2) = 0.1$, the level of silicon incorporation became 3.01. As the two samples contained boehmite evidenced from the XRD results, the values should be underestimated to some extent, especially for the former sample, which value should be far greater than 3. With the increase of silica concentration in the gel, the silicon incorporation degree descended rapidly. After $\gamma(\text{SiO}_2)$ in the gel was larger than 0.6, the value became less than 1. Fig. 3 compares the change of silicon content in product following that in gel based on the samples synthesized with different templates. Clearly, the silicon incorporation in the present work is obviously higher than that of

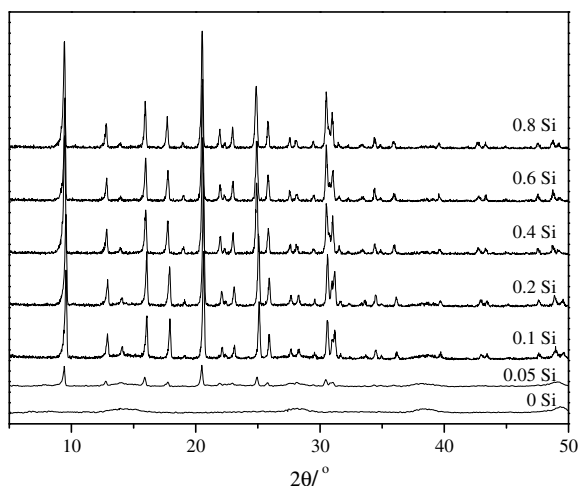


Fig. 2. XRD patterns of samples synthesized with different SiO_2 concentration in the initial gel ($2.0\text{DEA}:\gamma(\text{SiO}_2):1.0\text{Al}_2\text{O}_3:0.8\text{P}_2\text{O}_5:50\text{H}_2\text{O}$).

Table 2
Effect of SiO_2 concentration in the initial gel on synthesis

Sample	$\gamma(\text{SiO}_2)$	Relative crystallinity (%)	Molar composition	Si incorporation ^a
5	0.05	17	$\text{Si}_{0.04}\text{Al}_{0.72}\text{P}_{0.24}\text{O}_2$	2.93
6	0.1	86	$\text{Si}_{0.08}\text{Al}_{0.60}\text{P}_{0.32}\text{O}_2$	3.00
7	0.2	100	$\text{Si}_{0.10}\text{Al}_{0.55}\text{P}_{0.35}\text{O}_2$	1.97
8	0.4	97	$\text{Si}_{0.13}\text{Al}_{0.51}\text{P}_{0.36}\text{O}_2$	1.29
2	0.6	93	$\text{Si}_{0.15}\text{Al}_{0.49}\text{P}_{0.36}\text{O}_2$	1.05
9	0.8	94	$\text{Si}_{0.16}\text{Al}_{0.49}\text{P}_{0.35}\text{O}_2$	0.87

2.0DEA: $\gamma(\text{SiO}_2):1.0\text{Al}_2\text{O}_3:0.8\text{P}_2\text{O}_5:50\text{H}_2\text{O}$.

^a The level of silicon incorporation is defined as the molar ratio of $[\text{Si}/(\text{Si} + \text{Al} + \text{P})]_{\text{product}}/[\text{Si}/(\text{Si} + \text{Al} + \text{P})]_{\text{gel}}$.

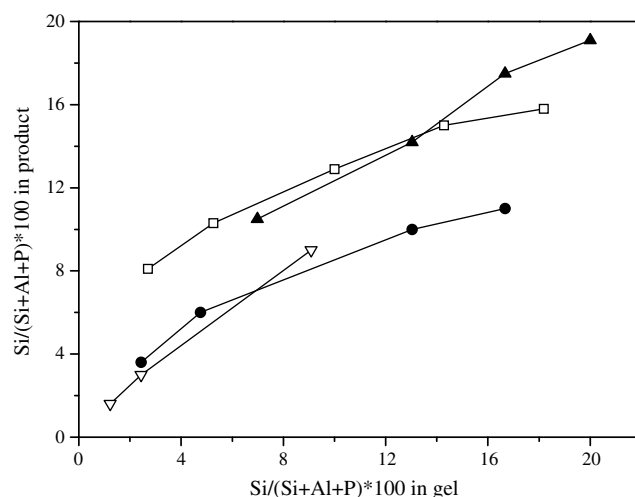


Fig. 3. Comparison of Si contents in SAPO-34 synthesized with different templates following those in the gel. □-DEA; ●-TEA (present work); ▽-TEAOH Ref. [15]; ▲-morpholine Refs. [31,32].

the samples synthesized with TEA and TEAOH [15]. This suggests that DEA can promote high silicon incorporation into the framework of SAPO-34. Prakash has also observed that SAPO-34 synthesized with morpholine as a template has the character of high silicon incorporation [6] and Fig. 3 shows that both values are very close [31,32].

3.2. SEM

The typical SEM photograph of SAPO-34 is presented in Fig. 4a. The cubic-like rhombohedra morphology could be clearly observed, which is quite similar to natural Chabasite. The crystal size is in the range of 3–7 μm . SEM photograph of pure SAPO-11 crystal obtained with DEA as a template is also given in Fig. 4b. Slice crystals aggregate into large spherical particles ranging from 16 to 20 μm .

3.3. ^{29}Si MAS NMR

^{29}Si MAS NMR was used to investigate the Si environments in the framework of SAPO-34. It can be seen that several peaks were present in the spectrum of sample 2,

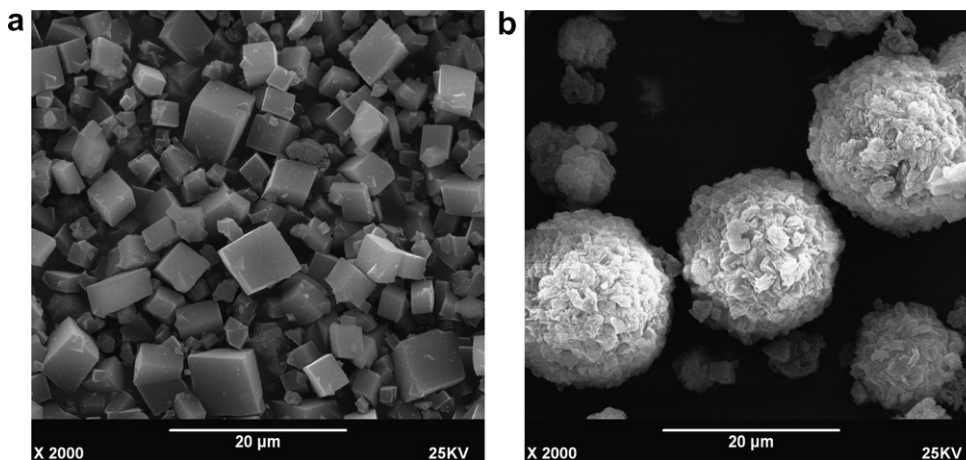


Fig. 4. SEM photographs of SAPO-34 (a) and SAPO-11 (b).

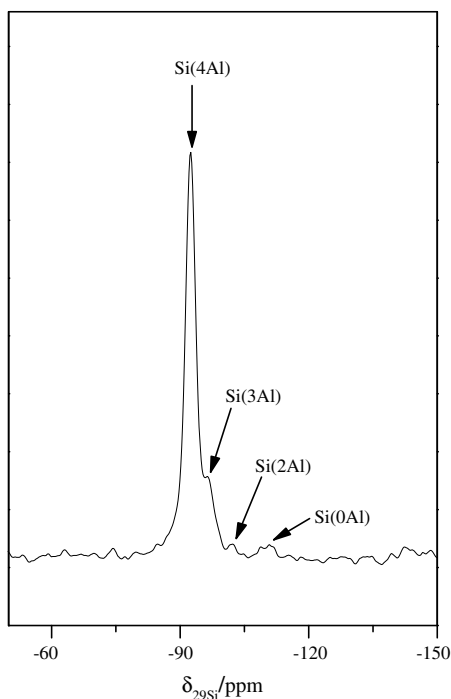


Fig. 5. ²⁹Si MAS NMR spectrum of sample 2.

as shown in Fig. 5. According to the literature [7], the strong peak at $\delta = -92.3$ ppm should be due to Si(4Al) specie; the peaks at $\delta = -96.6$ ppm and -100.6 ppm were ascribed to Si(3Al) and Si(2Al) species, respectively; the peak resulting from Si(0Al) environment appeared at $\delta = -110.9$ ppm. The presence of different Si environments are in agreement with the Si substitution mechanisms [23], i.e. SM2 (Si replaced P) and SM3 (Si replaced P&Al pairs).

3.4. FT-IR

FT-IR experiment indicates that the framework characteristic vibration peaks of SAPO-34 are comparable to those reported in the literature [7]: 1100 cm^{-1} ascribed to

the asymmetric stretch of O–P–O; 730 cm^{-1} arising from the symmetric stretch of O–P–O; 640 cm^{-1} due to the bend of double 6-ring; 575 cm^{-1} , 530 cm^{-1} and 480 cm^{-1} ascribed to the bend of PO₄, AlO₄, and SiO₄, respectively.

3.5. Thermal analysis

The TG-DTA profiles of sample 7 are described in Fig. 6a. TG result shows three weight losses (I, II, III) in the range of 50–900 °C. The first weight loss (I) of 1.50% in the low temperature range of 50–100 °C with an endothermic process is attributed to the water desorption from the sample. The second weight loss (II) of 13.23% between 100 and 430 °C with a strongly exothermic process is due to the combustion decomposition of template [25]. The third weight loss (III) of 1.60% at temperature higher than 430 °C with an exothermic process is likely associated with the further removal of organic residue occluded in the channels and cages of SAPO-34. It can be seen from the curves in Fig. 6a that there is no weight loss and exothermic peak associating with structural collapse until 900 °C. This suggests the high thermal stability of SAPO-34 synthesized in the present work, which is as good as those prepared with other templates [25,33–35].

As a comparison, thermal analysis of SAPO-34 synthesized with TEA as a template (sample 10) are also performed and shown in Fig. 6b. The ascriptions of all peaks are similar to those of sample 7 and the weight losses of each stage are listed in Table 3. Based on the topological structure of SAPO-34 molecular sieve, i.e. each unit cell containing three cages and 36 T sites, the average number of template per cage in two samples are calculated, with the result of 1.75 DEA for sample 7 and 1.00 TEA for sample 10.

As mentioned in the introduction, in addition to structure-directing and space-filling roles, organic template is very important for the compensation of framework charge. Barthomeuf et al. have demonstrated that the template can determine the maximum charge and govern the distribution of silicon in the framework [23]. They found that the value

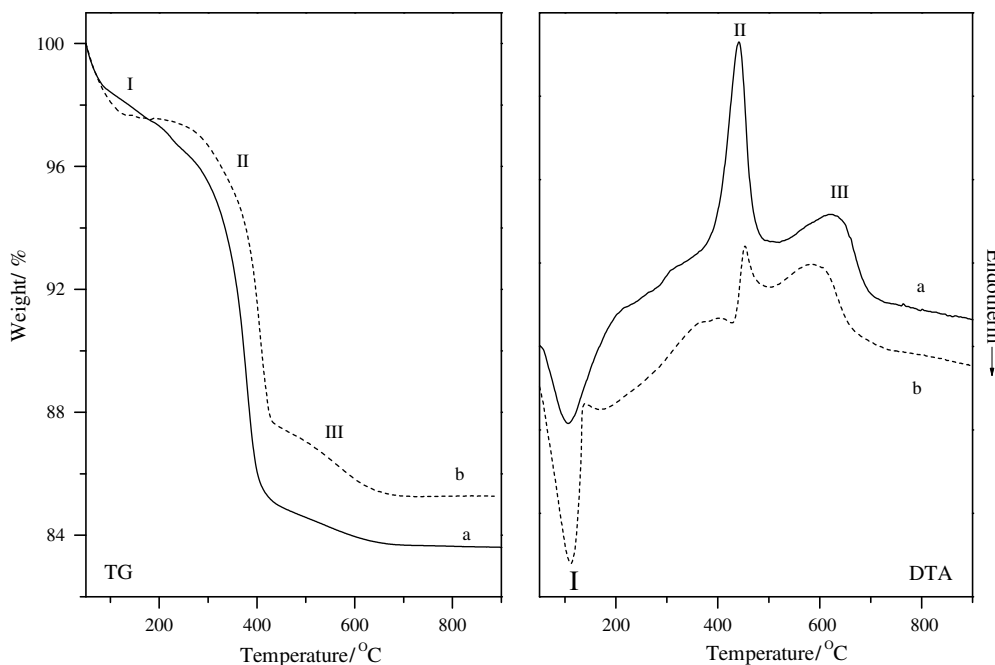


Fig. 6. TG-DTA profiles of SAPO-34 (a) sample 7 (b) sample 10.

Table 3
Thermal analysis results of SAPO-34

Sample	Weight loss (%)			Moles of template per cage
	I	II	III	
7	1.50	13.23	1.60	1.75
10 ^a	2.40	10.00	2.32	1.00

^a SAPO-34 synthesized using TEA as a template (gel molar ratio SiO₂/Al₂O₃ = 0.2).

of template molecules per cage in SAPO-34 with morpholine is 2.0 and the value for TEOH is 1.0. Moreover, it is well accepted that the use of organic templates gives rise to highly siliceous materials in the synthesis of Si–Al zeolites, due to the large size of these molecules, which limits their number in the zeolite cages. Among the four templates, which can be used in the synthesis of SAPO-34, TEOH and TEA are more bulky than DEA and morpholine. Therefore, the high incorporation of silicon with DEA as a template in the present work seems to be related to its smaller molecular size. The higher template concentration accommodated in each cage can compensate more framework charge and thus lead to the higher silicon content in the framework.

3.6. Hydrothermal stability

High-temperature steam treatment (800 °C, 24 h, 100% steam) was carried out in order to investigate the hydrothermal stability of SAPO-34 synthesized with DEA as a template, which is important for its practical catalytic application. The N₂ adsorption–desorption isotherms and textural information of samples are shown in Fig. 7 and Table 4, respectively.

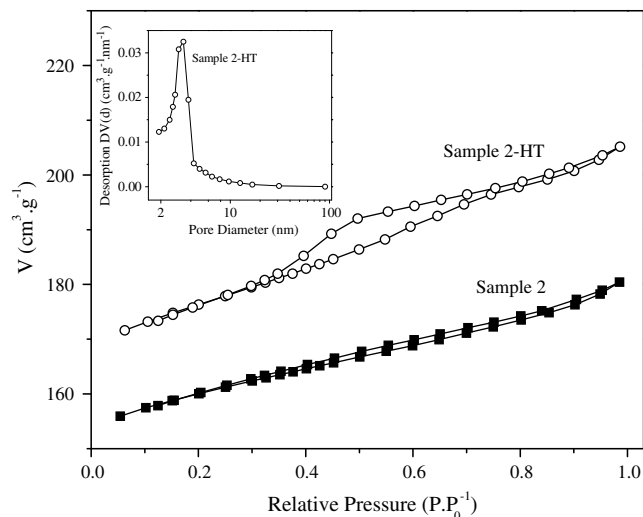


Fig. 7. N₂ adsorption–desorption isotherms of SAPO-34 (insert – the distribution of mesopore in sample 2-HT using BJH method from the desorption branch of the isotherm).

Table 4
Textual properties and relative crystallinity of SAPO-34 before and after hydrothermal treatment

Sample	Relative crystallinity (%)	Surface area (m ² /g)			Pore volume (ml/g)	
		S _{micro}	S _{ext}	S _{total}	V _{micro}	V _{total}
2	100	461	49	510	0.23	0.28
2-HT ^a	94	487	73	560	0.24	0.31

^a Hydrothermal treatment condition: 800 °C, 100% steam, 24 h.

According to the IUPAC classification [36], the isotherm of untreated sample 2 belongs to type I, and the BET surface area and pore volume were 510 m²/g and 0.28 ml/g,

respectively. After steam treatment, 94% relative crystallinity was preserved, and the total surface area and pore volume both increased by *ca.* 10%, indicating the good hydrothermal stability of SAPO-34 synthesized by DEA. The changes should be resulted from the appearance of mesoporous structure in sample 2-HT, as deduced from the hysteresis loop between $P/P_0 = 0.4\text{--}0.8$ in the isotherm. The phenomenon is common in zeolites. Mesoporous structure appeared together with the occurrence of dealumination during the hydrothermal treatment of zeolites, such as Y [37,38] and ZSM-5 [39]. However, for SAPO molecular sieves slight desilicization, not dealumination, may happen during the steam treatment. Our previous work has demonstrated that Si was rich on the surface of SAPO-34 crystals after steam treatment (XPS analysis) [40]. This means that part of Si migrated from the interior of the crystal to the surface in the presence of high-temperature steam. During the course of Si migration, P and Al migration may also occur to a certain extent, which thus caused the formation of mesopores.

3.7. Catalytic performance

The catalytic performance of SAPO-34 in MTO reaction was tested. Fig. 8 gives the methanol conversion and selec-

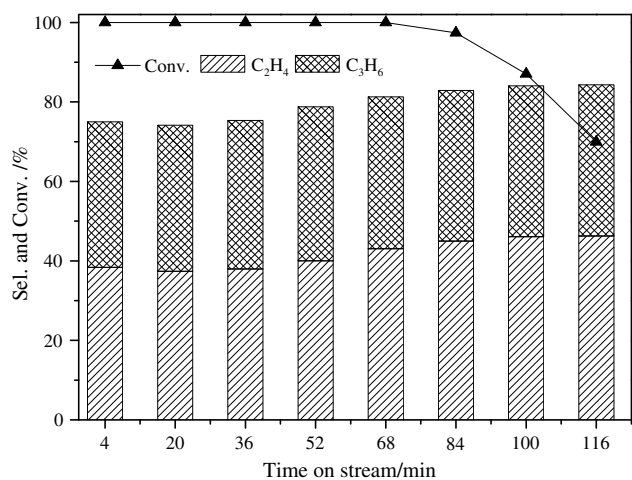


Fig. 8. Conversion and selectivity of C₂H₄ and C₃H₆ with time on sample 1.

Table 5
MTO reaction results of SAPO-34 samples with different silicon content^a

Sample	Si fraction in product	Lifetime (min) ^b	Selectivity (wt%) ^c							
			CH ₄	C ₂ H ₄	C ₂ H ₆	C ₃ H ₆	C ₃ H ₈	C ₄ ⁺	C ₅ ⁺	C ₂ H ₄ + C ₃ H ₆
7	0.10	68	1.2	44.0	0.8	37.5	2.6	10.9	3.1	81.5
8	0.13	52	1.2	41.8	1.0	38.2	3.5	11.7	2.6	80.0
2	0.15	52	1.3	41.0	1.1	37.8	4.1	11.7	3.0	78.8
9	0.16	36	1.2	37.0	1.2	37.0	6.0	13.9	3.7	74.0
2-HT	0.15	36	1.9	43.0	1.4	35.1	3.1	12.7	2.7	78.1
11 ^d	0.10	82	1.4	41.1	0.6	39.9	2.5	11.8	2.8	81.0

^a Test condition: WHSV = 4 h⁻¹, T = 450 °C, 40 wt% methanol solution.

^b The lifetime is defined as the reaction duration with 100% methanol conversion.

^c The highest selectivity of (C₂H₄ + C₃H₆) under 100% methanol conversion.

^d SAPO-34 synthesized with TEA as a template ($n(\text{SiO}_2)/n(\text{Al}_2\text{O}_3) = 0.6$ in the gel, product composition Si_{0.10}Al_{0.49}P_{0.41}).

tivity of C₂H₄ and C₃H₆ with time on sample 1. As presented in the figure, the selectivity of light olefins (C₂H₄ + C₃H₆) rises with time and can reach the maximum of 81.5% under 100% methanol conversion. Ethylene selectivity increases with time, whereas propylene selectivity levels off. The change of ethylene selectivity could be related to the coking effect, which reduced the pore size of SAPO-34 and thus increased the ethylene selectivity [12,41,42].

Table 5 presents the results of MTO reaction on SAPO-34 samples with different silicon content. With the increase of silicon content in SAPO-34, the catalysts lifetime and the olefins selectivity decreased, and propane selectivity augmented gradually. This result should be associated with the increased acidity and acid amount in SAPO-34 with higher Si content, which caused the enhancement of coke formation (short catalyst lifetime) and hydride transfer reaction (high propane selectivity). The effect of hydrothermal treatment on the catalytic performance of SAPO-34 was also tested. As shown in Table 5, the olefins selectivity of sample 2-HT nearly kept the same as that of the fresh sample except the lifetime became shorter.

The MTO result of SAPO-34 synthesized with TEA (sample 11, gel molar ratio SiO₂/Al₂O₃ = 0.6, product composition Si_{0.10}Al_{0.49}P_{0.41}) is given in Table 5. As sample 11 has the similar Si content as that of sample 7, the comparison of reaction properties between these two samples should be more reasonable. It can be seen that the highest selectivity of olefins on both samples are close, but SAPO-34 synthesized with TEA has longer lifetime than that with DEA.

4. Conclusions

The synthesis of SAPO-34 using DEA as a template was investigated in detail. Pure SAPO-34 was successfully synthesized and the optimal condition was obtained at $n(\text{DEA})/n(\text{Al}_2\text{O}_3) \geq 1.5$ and $n(\text{SiO}_2)/n(\text{Al}_2\text{O}_3) > 0.1$ in the initial gel. Too much DEA in the gel [$n(\text{DEA})/n(\text{Al}_2\text{O}_3) > 3$] would cause obvious decrease of crystallinity and crystal yield. High silicon incorporation into the framework of SAPO-34 with DEA as a template was found and possibly relates to the template's smaller molecular size

from the thermal analysis – 1.75 molecules per cage for DEA, whereas only 1.0 per cage for TEA. Furthermore, SAPO-34 showed high hydrothermal stability, as evidenced from the results of XRD and N₂ physisorption isotherms.

SAPO-34 behaved good catalytic performance in MTO reaction and the maximum of 81.5% light olefins (C₂H₄ + C₃H₆) selectivity under 100% methanol conversion was obtained. With the increase of silicon content in SAPO-34, the catalysts lifetime and olefins selectivity decreased gradually. Sample after high-temperature steam treatment possessed similar olefins selectivity as that of the fresh sample, except the lifetime became shorter.

References

- [1] S.T. Wilson, B.M. Lok, C.A. Messina, T.R. Cannan, E.M. Flanigen, *J. Am. Chem. Soc.* 104 (1982) 1146.
- [2] B.M. Lok, C.A. Messina, R.L. Patton, R.T. Gajek, T.R. Cannan, E.M. Flanigen, *J. Am. Chem. Soc.* 106 (1984) 6092.
- [3] M. Stöcker, *Micropor. Mesopor. Mater.* 29 (1999) 3.
- [4] J.F. Haw, W.G. Song, D.M. Marcus, J.B. Nicholas, *Acc. Chem. Res.* 36 (2003) 317.
- [5] H.O. Pastore, S. Coluccia, L. Marchese, *Annu. Rev. Mater. Res.* 35 (2005) 351.
- [6] A.M. Prakash, S. Unnikrishnan, *J. Chem. Soc. Faraday Trans.* 90 (1994) 2291.
- [7] J. Tan, Z.M. Liu, X.H. Bao, X.C. Liu, X.W. Han, C.Q. He, R.S. Zhai, *Micropor. Mesopor. Mater.* 53 (2002) 97.
- [8] Ø.B. Vistad, D.E. Akporiaye, F. Taulelle, K.P. Lillerud, *Chem. Mater.* 15 (2003) 1639.
- [9] J.Q. Chen, A. Bozzano, B. Glover, T. Fuglerud, S. Kvisle, *Catal. Today* 106 (2005) 103.
- [10] X.C. Wu, M.G. Abraha, R.G. Anthony, *Appl. Catal. A* 260 (2004) 63.
- [11] D.R. Dubois, D.L. Obrzut, J. Liu, J. Thundimadathil, P.M. Adekanattu, J.A. Guin, A. Punnoose, M.S. Seehra, *Fuel Proc. Technol.* 83 (2003) 203.
- [12] W.G. Song, H. Fu, J.F. Haw, *J. Am. Chem. Soc.* 123 (2001) 4749.
- [13] M. Kang, *J. Mol. Catal. A* 160 (2000) 437.
- [14] D. Chen, K. Moljord, T. Fuglerud, A. Holmen, *Micropor. Mesopor. Mater.* 29 (1999) 191.
- [15] S. Wilson, P. Barger, *Micropor. Mesopor. Mater.* 29 (1999) 117.
- [16] M. Popova, Ch. Minchev, V. Kanazirev, *Appl. Catal. A* 169 (1998) 227.
- [17] Z.M. Cui, Q. Liu, W.G. Song, L.J. Wan, *Angew. Chem. Int. Ed.* 45 (2006) 6512.
- [18] M. Hunger, M. Seiler, A. Buchholz, *Catal. Lett.* 74 (2001) 61.
- [19] W.G. Song, J.F. Haw, J.B. Nicholas, C.S. Heneghan, *J. Am. Chem. Soc.* 122 (2000) 10726.
- [20] B. Arstad, S. Kolboe, *Catal. Lett.* 71 (2001) 209.
- [21] B. Arstad, S. Kolboe, *J. Am. Chem. Soc.* 123 (2001) 8137.
- [22] B.M. Lok, T.R. Cannan, C.A. Messina, *Zeolites* 3 (1983) 282.
- [23] R. Vomscheid, M. Briend, M.J. Peltre, P.P. Man, D. Barthomeuf, *J. Phys. Chem.* 98 (1994) 9614.
- [24] B.M. Lok, C.A. Messina, R.L. Patton, R.T. Gajek, T.R. Cannan, E.M. Flanigen, US Patent 4440871, 1984.
- [25] E. Dumitriu, A. Azzouz, V. Hulea, D. Lutic, H. Kessler, *Micropor. Mater.* 10 (1997) 1.
- [26] L. Marchese, A. Frache, E. Gianotti, G. Martra, M. Causà, S. Coluccia, *Micropor. Mesopor. Mater.* 30 (1999) 145.
- [27] Y.X. Wei, D.Z. Zhang, Z.M. Liu, B.L. Su, *J. Catal.* 238 (2006) 46.
- [28] C.Q. He, Z.M. Liu, G.Y. Cai, L.X. Yang, Z.Z. Wang, J.S. Luo, X.S. Pan, Z.Q. Ge, Y.J. Chang, R.M. Shi, CN Patent 1096496, 1994.
- [29] Y.Y. Zheng, T.L. Yang, X.H. Zhou, S.K. Shen, *J. Fuel Chem. Technol.* 27 (1999) 139.
- [30] M.M.J. Treacy, J.B. Higgins, in: *Collection of Simulated XRD Powder Patterns for Zeolites*, Elsevier, Amsterdam, 2001.
- [31] Z.D. Zhu, M. Hartmann, L. Kevan, *Chem. Mater.* 12 (2000) 2781.
- [32] S. Ashtekar, S.V.V. Chilukuri, D.K. Chakrabarty, *J. Phys. Chem.* 98 (1994) 4878.
- [33] P.T. Barger, D.A. Lesch, *Arabian J. Sci. Eng.* 21 (1996) 263.
- [34] Y. Watanabe, A. Koiwai, H. Takeuchi, S. Hyodo, S. Noda, *J. Catal.* 143 (1993) 430.
- [35] H.X. Liu, Z.K. Xie, C.F. Zhang, Q.L. Chen, *Chin. J. Chem. Phys.* 16 (2003) 521.
- [36] K.S.W. Sing, D.H. Everett, R.A.W. Haul, L. Moscou, J. Pierotti, J. Rouquerol, T. Siemieniowska, *Pure Appl. Chem.* 57 (1985) 603.
- [37] A.H. Janssen, A.J. Koster, K.P. de Jong, *Angew. Chem. Int. Ed.* 40 (2001) 1102.
- [38] S. van Donk, A.H. Janssen, J.H. Bitter, K.P. de Jong, *Catal. Rev.* 45 (2003) 297.
- [39] J.C. Groena, J.A. Moulijna, J. Pérez-Ramírez, *Micropor. Mesopor. Mater.* 87 (2005) 153.
- [40] Z.M. Liu, X.Y. Huang, C.Q. He, Y. Yang, L.X. Yang, G.Y. Cai, *Chin. J. Catal.* 17 (1996) 540.
- [41] W.G. Song, H. Fu, J.F. Haw, *J. Phys. Chem. B* 105 (2001) 12839.
- [42] B. Arstad, J.B. Nicholas, J.F. Haw, *J. Am. Chem. Soc.* 126 (2004) 2991.